Anomalous Rashba spin-orbit interaction in InAs/GaSb quantum wells

Jun Li and Kai Chang*
SKLSM, Institute of Semiconductors, Chinese Academy of Sciences, P. O. Box 912, Beijing 100083, China

G. Q. Hai
Instituto de Física de São Carlos, Universidade de São Paulo, 13560-970 São Carlos, São Paulo, Brazil

K. S. Chan
Department of Physics and Materials Science, City University of Hong Kong, Hong Kong, China

We investigate theoretically the Rashba spin-orbit interaction in InAs/GaSb quantum wells (QWs). We find that the Rashba spin-splitting (RSS) depends sensitively on the thickness of the InAs layer. The RSS exhibits nonlinear behavior for narrow InAs/GaSb QWs and the oscillating feature for wide InAs/GaSb QWs. The nonlinear and oscillating behaviors arise from the weakened and enhanced interband coupling. The RSS also show asymmetric features respect to the direction of the external electric field.

PACS numbers: 78.40.Ri, 42.70.Qs, 42.79.Fm

InAs/GaSb superlattices (SLs) and quantum wells (QWs) have attracted intensive attention in the past decades due to their potential application in nanoelectronics and remarkable electronic properties, e.g., the infrared detector and laser diode, as well as interband tunneling diodes and transistors[1,2,3,4]. An interesting feature of this broken-gap structure is that the top of the valence band of GaSb lies above the bottom of the conduction band of InAs. A two-dimensional electron gas (2DEG) in the InAs layer can coexist with a two-dimensional hole gas in the GaSb layer since the electron can move across the InAs/GaSb interface from the valence band of GaSb to the conduction band of InAs, consequently leading to a semimetallic phase[1,5]. The energy spectrum exhibits an anticrossing behavior between the top valence subband and the lowest conduction subband at finite in-plane momentum when the lowest conduction subband in InAs layer lies below the top valence subband in GaSb layer[6]. The hybridized gap caused by the anticrossing was observed experimentally[7], and leads to the semiconducting behavior of system. Recently, by utilizing the unique characteristics of the InAs/GaSb/AlSb system, e.g., the strong spin-orbit interaction (SOI) in InAs and GaSb and the high electron mobility of InAs, it may be possible to realize high-speed spintronic devices, e.g., Rashba spin filters[8,9,10], a spin field effect transistor[11] and a high-frequency optical modulator utilizing spin precession[12]. The SOI also has a significant influence on the spin relaxation of electrons in semiconductors and could be used to generate the spin current.

In this Letter, we investigate theoretically the Rashba spin-splitting (RSS) in undoped InAs/GaSb quantum wells sandwiched by AlSb barriers by solving the eight-band Kane Hamiltonian[13,14] and Poisson equation self-consistently. We find a spontaneous RSS that arises from the interface contribution in the absence of external electric field, and RSS is asymmetric with respect to the direction of external electric field. It is interesting to note that RSS exhibits distinct behavior, i.e., nonlinear and oscillating feature as a function of the in-plane momentum, at small and large thicknesses of InAs layers due to the interband coupling and hybridization between the conduction band and the valence band.

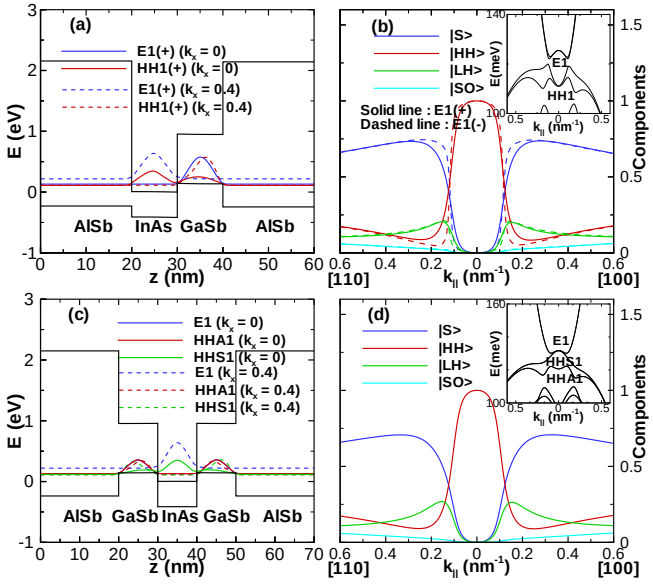

FIG. 1: (a) Band profile and the probability density distribution of E1(+) (blue), HH1(+) (red) subband in InAs/GaSb ASQW at $k_{\parallel} = 0$ (solid line) and $k_{\parallel} = 0.4\ nm^{-1}$ (dashed line), ($L_{InAs} = 10\ nm, L_{GaSb} = 10\ nm$). (b) The four band-edge state components, $|S\rangle$ (blue), $|HH\rangle$ (red), $|LH\rangle$ (green) and $|SO\rangle$ (cyan) as a function of in-plane wavevector of E1 band. The solid and dashed line denote the spin up (E1(+)) and spin down(E1(-)) state, respectively. The inset shows the calculated band structure. (c) and (d), the same as (a) and (b), but for a GaSb/InAs/GaSb SQW.

We consider an undoped InAs/GaSb quantum well (grown on the [001] plane) shown schematically in Fig. 1(a). If an external electric field F is applied along the

direction perpendicular to the QW plane, an external electric field term $V_E(z) = eFz$ should be added to the total Hamiltonian. When the layer thickness or the external electric field is sufficiently large so that the bottom of the lowest conduction subband in InAs layer falls below the top of the highest valence subband in GaSb layer, electrons could transfer from GaSb layer to InAs layer, thus induced an internal electrostatic potential $V_{in}(z)$ in InAs and GaSb layers[15]. The total Hamiltonian writes as $H = H_k + V_E(z) + V_{in}(z)$ including the external and internal electrostatic potential. A self-consistent iteration procedure is performed until $V_{in}(z)$ is stable. The Kane parameters of materials used in our calculation are obtained from Ref. 16.

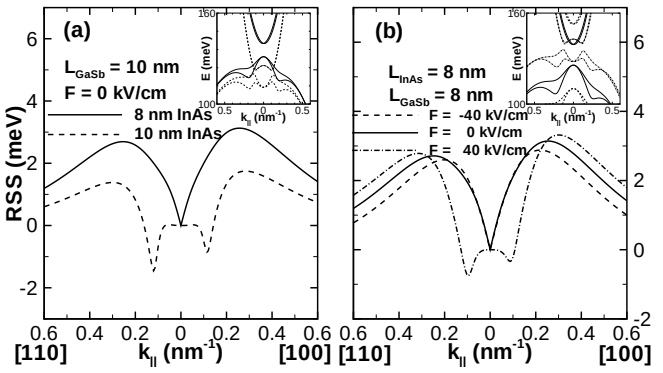

FIG. 2: (a)Rashba spin-splitting of E1 band as a function of the in-plane momentum in the absence of external electric field for different thicknesses of InAs layer. (b) The same as (a), but for different external electric fields. The insets depict the band structure near the band gap.

Fig. 1 (a) shows schematically the self-consistent band profile of a 10 nm-10 nm InAs/GaSb asymmetric chemical multilayer QW (ASQW) at $k_\parallel = 0$. The energy dispersion of the ASQW obtained from the self-consistent calculation is plotted in the inset of Fig. 1(b). From the energy dispersion, we can find that the energy dispersion of the lowest (highest) conduction (valence) subband shows a minimum (maximum) at a finite $k_\parallel^a$, i.e., anticrossing behavior, since the bottom of the lowest electron subband in the InAs layer lies below the top of the highest heavy-hole subband in the GaSb layer. A spin-dependent hybridized gap($\sim$3 meV) at the anticrossing point forms due to the strong mixing effect of the InAs electron state and the GaSb hole state. In this QW, the concentration of electrons transferred from GaSb layer to InAs layer is found to be at the order of 1.9×10^{-11} cm^{-2}, which induces a 7 meV bending down (up) in the profile of InAs's conduction band (GaSb's valence band) near the interface. The small band-bending only change the results slightly and shifts $k_\parallel^a$ to a smaller value. In Fig. 1(b), we plot the four components of the E1 state as a function of $k_\parallel$. The dominant component of E1 states (E1(+) and E1(-)) experiences a crossover from $|HH\rangle$ to $|S\rangle$ when the in-plane momentum $k_\parallel$ sweeps across the anticrossing point $k_\parallel^a$. Meanwhile, the dominant component of the HH1 band varies from electron-like to hole-like feature. This feature can also be demonstrated in Fig. 1(a) in which we also plot the density distribution of the E1(+) and HH1(+) at $k_\parallel = 0$ and 0.4 nm^{-1}. At $k_\parallel = 0$, the E1 (HH1) state is mostly heavy-hole-like (electron-like) and therefore localizes in the GaSb (InAs) layer. At $k_\parallel > k_\parallel^a$, the two anticrossing subbands E1 and HH1 exchange their main characteristics, so the density distribution of E1(HH1) state localizes in InAs(GaSb) layer. Fig. 1 (c) and (d) plot the situation of a symmetric chemical multilayer QW (SQW). In this symmetric structure, the internal electrostatic potential is symmetric respect to the center of InAs layer. Thus there is no RSS existing, and the components of the two spin branches of E1 are identical in Fig. 1(d).

In Fig. 2 (a) we plot the Rashba spin-splitting (RSS) of the lowest conduction subband (E1) as a function of the in-plane momentum at fixed thicknesses of the InAs and GaSb layers. As shown in the insets, the energy bands of narrow QW, e.g., 8 nm InAs layer with 10 nm GaSb layer, manifest a normal semiconductor phase since the strong quantum confinement pushes the lowest conduction subband to a higher energy. The RSS in this QW is a nonlinear function of in-plane wave vector, just as the RSS in biased narrow band gap semiconductor QWs we reported elsewhere before[14]. Interesting difference between this work and the previous work[14] is that there exist a spontaneous RSS in the InAs/GaSb QW in the absence of external electric fields, since it arises mainly from the asymmetric potential profile of InAs/GaSb QW, i.e., the asymmetric interband coupling at the left and right interfaces for InAs and GaSb layers. This is clearly demonstrated by the disappearing of the spontaneous RSS in the GaSb/InAs/GaSb SQW (see Fig. 1(c) and (d)). Besides the nonlinear RSS, one can also see an oscillating RSS of the E1 band in a wider QW, e.g., the QW of 10 nm InAs layer with 10 nm GaSb layer, in which an anticrossing occurs in the energy spectrum (see the inset of Fig. 2 (a)). A sharp drop of RSS corresponding to the anticrossing point $k_\parallel^a$ appears. It is interesting to see that the RSS changed its sign near the anticrossing point. Obviously the sign change of RSS corresponds to the cross of the two spin branches. In addition, the RSS is anisotropic with respect to different $k_\parallel$ direction, e.g., [100] and [110] direction (see Fig. 2). The anisotropy of RSS comes from the anisotropy of valence bands of InAs/GaSb QW through interband coupling.

Fig. 2 (b) displays the RSS of an InAs/GaSb quantum well as a function of the in-plane momentum for different external perpendicular electric fields. This figure shows that the RSS is heavily controlled by the external electric field. This behavior of RSS can be explained by the interplay between the asymmetric interface contribution and the interband coupling induced by the external electric field. In Fig. 2 (b), if an external electric field is applied parallel to the positive direction of the z axis, the energy of the conduction subbands decreases while

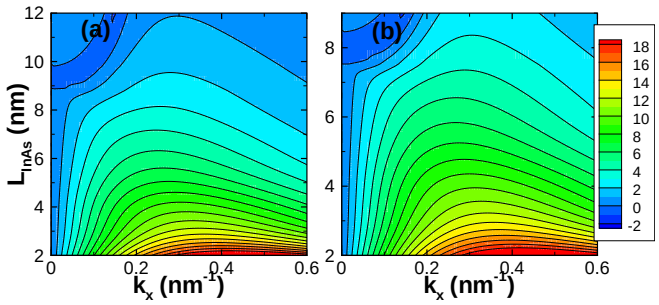

FIG. 3: (a) Contour plot of self-consistently calculated RSS of E1 band as a function of the in-plane momentum and the thickness of the InAs layer without external electric field. (b) The same as (a), but with an external electric field $F = 40\ kV/cm$. In each panel the thickness of GaSb layer is fixed at 8 nm.

the energy of the valence subbands increases. Thus, the anticrossing behavior occurs or is enhanced even for QW with a narrow width InAs layer that exhibits a normal-semiconductor phase in zero electric field[17]. A valley of RSS appears once an anticrossing happens. The energy difference between the E1 and HH1 subbands is increased when the external electric field is applied antiparallel to the z axis. Therefore the anticrossing behavior is weakened and even smeared out. Compared to the conventional type-I QW, RSS in the type-II InAs/GaSb broken-gap QW exhibits unique features, i.e., nonlinear and oscillating behaviors which can be tuned by the external electric field.

For the wide ASQW case (see Figs. 2 (a) and (b)), the internal electrostatic potential induced by charge transfer tends to weaken the coupling between the conduction subbands in InAs layer and the valence subbands in GaSb layer, i.e., the internal electric field compensates partly the external electric field, and shifts the anticrossing point to a smaller $k_{\|}$. In normal semiconductor phases of undoped InAs/GaSb QW, the charge transfer process doesn't happen, therefore the internal electrostatic potential disappears.

Figs. 3 (a) and (b) describe the RSS as function of the in-plane momentum and the thickness of the InAs layer in zero and finite electric field. From this contour plot one can see more clearly that the RSS shows a nonlinear feature for the narrow InAs layer, and an oscillating behavior at large thickness of InAs layer. The nonlinear behavior arises from the interface contribution which also depends on the interband coupling[14]. The oscillation of RSS is caused by the strong mixing between the conduction subband E1 and the heavy-hole subband HH1. Interestingly, this oscillating behavior of RSS can be enhanced by an electric field, e.g., $F = 40\ kV/cm$, (see Fig. 3 (b)). Note that there is a critical thickness of the InAs layer L_c, the RSS exhibits oscillating features corresponding to the different phases when $L > L_c$.

Fig.4 (a) displays the phase diagram of InAs/GaSb QWs for different external electric fields. This figure indicates that the critical thickness of the InAs layer decreases as the thickness of GaSb layer increases, and tends to saturate at different thicknesses determined by the external electric fields (see Fig. 4 (a)). Positive external electric fields decrease the critical thickness, while negative external electric fields increase the critical thickness. Fig. 4 (b) gives the critical thickness of InAs layer and the critical electric field for different thicknesses of the GaSb layers. The critical electric fields saturate at different valyes for different thicknesses of the GaSb layers.

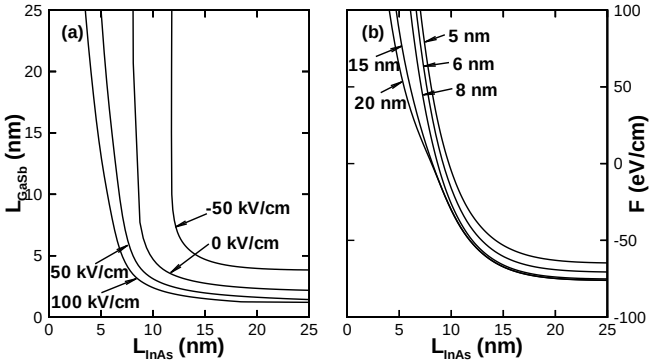

FIG. 4: (a) The phase diagram of InAs/GaSb QWs as function of the thickness of InAs and GaSb layers for different electric fields. (b) The Same as (a), but as function of the thickness of InAs layer and the external electric field for different thicknesses of the GaSb layers.

In summary, we theoretically investigated Rashba spin-orbit interaction in InAs/GaSb asymmetric chemical multilayer QWs. We found a spontaneous RSS that arises from the interface contribution induced by the asymmetric structure of the QW. The RSS exhibits distinct behaviors, i.e., nonlinear and oscillating behavior, depending on the thickness of the QW and the external electric field. The oscillating RSS comes from the strong interband mixing between the lowest InAs conduction and the highest valence GaSb subbands. This crossover between two distinct behaviors can be tuned by the thicknesses of the InAs or GaSb layers and the external electric field. The unique features of RSS in InAs/GaSb QWs could provide us an interesting way to manipulate the electron spin and construct spintronic devices.

Acknowledgments

This work was supported by the NSFC Grant No. 60525405 and the knowledge innovation project from CAS, , City University of Hong Kong Strategic Research Grant (project no. 7002029). GQH was supported by FAPESP and CNPq (Brazil).

* Corresponding author:kchang@red.semi.ac.cn

[1] G. A. Sai-Halasz, R. Tsu, and L. Esaki, Appl. Phys. Lett. **30**, 651 (1977); G. A. Sai-Halasz, L. Esaki, and W. A. Harrison, Phys. Rev. B **18**, 2812 (1978).

[2] J. R. Södeström, D. H. Chow and T. C. McGill, Appl. Phys. Lett. **55**, 1094 (1989); L. F. Luo, R. Beresford and W. I. Wang, Appl. Phys. Lett. **55**, 2023 (1989).

[3] D. Z-Y. Ting, D. A. Collins, E. T. Yu, D. H. Chow and T. C. McGill, Appl. Phys. Lett. **57**, 1257 (1990).

[4] M. P. Houng, Y. H. Wang, S. L. Shen, J. F. Chen and A. Y. Cho, Appl. Phys. Lett. **60**, 713 (1992).

[5] J. Luo, H. Munekata, F. F. Fang, and P. J. Stiles, Phys. Rev. B **41**, 7685 (1990).

[6] Y.-C. Chang and J. N. Schulman, Phys. Rev. B **31**, 2069 (1985); J.-C. Chiang, S.-F. Tsay, Z. M. Chau, and I. Lo, Phy. Rev. Lett **77**, 2053 (1996); S. de-Leon, L. D. Shvartsman, and B. Laikhtman, Phy. Rev. B **60**, 1861 (1999); A. Zakharova, S. T. Yen, and K. A. Chao, Phy. Rev. B **66**, 085312 (2002).

[7] M. J. Yang, C. H. Yang, B. R. Bennett, and B. V. Shanabrook, Phy. Rev. Lett. **78**, 4613 (1997); M. Lakrimi, S. Khym, R. J. Nicholas, D. M. Symons, F. M. Peeters, N. J. Mason, and P. J. Walker, Phy. Rev. Lett. **79**, 3034 (1997); L. J. Cooper, N. K. Patel, V. Drouot, E. H. Linfield, D. A. Ritchie, and M. Pepper, Phy. Rev. B **57**, 11915 (1998); T. P. Marlow, L. J. Cooper, D. D. Arnone, N. K. Patel, D. M. Whittaker, E. H. Linfield, D. A. Ritchie, and M. Pepper, Phy. Rev. Lett. **82**, 2362 (1999).

[8] A. Voskoboynikov, S. S. Lin, C. P. Lee, and O. Tretyak, J. Appl. Phys. **87**, 387 (2000).

[9] T. Koga, J. Nitta, H. Takayanagi, and S. Datta, Phys. Rev. Lett. **88**, 126601 (2002).

[10] D. Z. -Y. Ting and X. Cartoixa, Appl. Phys. Lett. **81**, 4198 (2002).

[11] S. Datta and B. Das, Appl. Phys. Lett. **56**, 665 (1990).

[12] S. Hallstein, J. D. Berger, M. Hilpert, H.C. Schneider, W. W. Rühle, F. Jahnke, S.W. Koch, H. M Gibbs, G. Khitrova, and M. Oestreich, Phys. Rev. B **56**, 7076 (1997).

[13] M. G. Burt, J. Phys.: Condens. Matter **4**, 6651 (1992); B. A. Foreman, Phys. Rev. B **56**, R12748 (1997); T. Darnhofer and U. Rossler, *ibid.* **47**, 16020 (1993).

[14] W. Yang and Kai Chang, Phys. Rev. B, **73**, 113303 (2006); W. Yang and Kai Chang, *ibid.* **74**, 193314 (2006).

[15] G. Bastard, E. E. Mendez, L. L. Chang, and L. Esaki, J. Vac. Sci. Technol. **21**, 531 (1982).

[16] I. Vurgaftmana, J. R. Meyer and L. R. Ram-Mohan, J. Appl. Phys. **89**, 5815 (2001).

[17] Y. Naveh and B. Laikhtman, Appl. Phys. Lett. **66**, 713 (1995).

[18] H. B. de Carvalho, et al., Phys. Rev. B **74**, 041305 (2006).